

# Regulation and Compensation of Source Harmonics for the Boost Converter–Based Power Factor Precompensator

G. Escobar, A.M. Stanković\*  
 Dept Electrical and Computer Eng  
 Northeastern University  
 {gescobar, astankov}@ece.neu.edu

D.J. Perreault  
 Dept. of Electrical Engineering and Computer  
 Science  
 Massachusetts Institute of Technology  
 djperrea@mit.edu

*Abstract*—In this paper we present an adaptive controller for the boost-based power factor precompensator which guarantees fast regulation of the output voltage towards a desired constant value with a power factor close to unity. This twofold control objective is fulfilled even in the presence of harmonics on the voltage source and uncertainties on the system parameters and load. The key for the solution to this problem is to express the model in terms of the input current instead of the inductor current. The resulting controller is reduced, through transformations, to the cascade interconnection of two controllers, namely the inner and the outer control loop. It is shown that while the latter turns out to be a simple lead–lag plus integration, the former is composed mainly of second order filters tuned at the frequencies of the considered harmonics and with transfer functions that follow a well defined pattern. Simulations are provided to assess the performance of the proposed controller.

*Keywords*—AC-DC power conversion, power supplies, reactive power, dissipative systems, adaptive control, nonlinear systems.

## I. INTRODUCTION

REGULATION of switched power converters is an active area of research, both in the power electronics area [2], [3] and in automatic control theory [4], [5]. This is due to the fact that power converters are, generally speaking, a ubiquitous power source whose applicability ranges from electrodomeotics and digital computers to industrial electronics and sophisticated communications equipment. From the theoretical viewpoint, they also constitute an interesting class of discontinuous nonlinear systems regulated by means of a commanded switch position function. These features make switched power converters attractive for both theoretical and practically-oriented studies.

In this paper we explore the performance enhancement of Power Factor Precompensators (PFP) via adaptive nonlinear control techniques. The topology of the PFP circuit studied in the present work consists of a *diode bridge* and associated boost converter. This circuit is the most widely employed of the family of PFP's even though it exhibits certain drawbacks such as the slight deformation in the signal around the zero crossing.

We propose an *nonlinear feedback controller* designed following a dissipativity approach to which adaptation has been added to cope with parametric uncertainties. The closed loop performance accomplish the twofold control objective: first, to achieve a nearly unit power factor at the input of the converter, and second, to achieve efficient load voltage regulation to a desired constant level. By defining a reference signal tracking problem on the input current of the converter, the power fac-

tor can be made very close to unity as long as the tracked current signal is a scaled replica of the input voltage. Hence, the source will see the controlled system as the same equivalent resistor at each harmonic frequency. Our solution considers the main parameters of the system (the capacitance and the inductance) and of the applied load as unknowns; we also allow for harmonics in the voltage source. While in the case of known system parameters the problem can be solved with conventional control techniques, the required bandwidth of the current control loop can easily become excessive. As an alternative, we developed a controller that utilizes the information about the structure of the system and disturbances to improve performance, and to significantly reduce the bandwidth of the current loop.

The use of a system model representation in terms of the input current, instead of the usual inductor current, is instrumental for our developments. This allows us to treat the problem of harmonic contents in the input voltage in a more natural way. The input voltage can then be expressed in the form of Fourier series, where the coefficients are unknown constants. The resulting controller will have a familiar and simple form which is suitable for implementation, where the most relevant feature is the introduction of a bank of second order filters, with resonant frequencies corresponding to the harmonic under consideration.

## II. SWITCH-REGULATED BOOST CONVERTER AS A PFP

In this section we formulate the control problem of the PFP whose circuit is shown in Fig. 1.

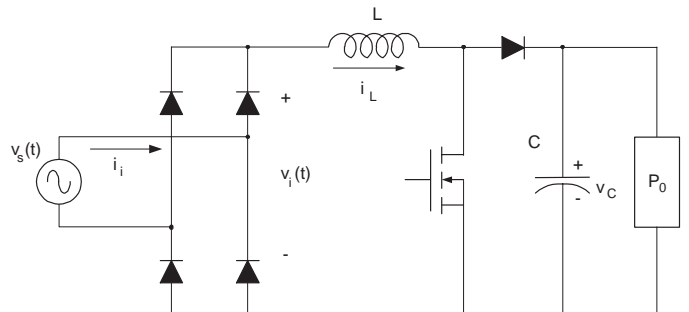


Fig. 1. Switch-regulated PFP Boost circuit

\*Corresponding author.

The differential equations describing the circuit dynamics are

$$\begin{aligned} L \frac{d}{dt} i_L &= -uv_C + v_i \\ C \frac{d}{dt} \left( \frac{v_C^2}{2} \right) &= uv_C i_L - P_0 \end{aligned} \quad (1)$$

where  $i_L$  and  $v_C$  are the inductor current and the capacitor voltage variables, respectively; notice that  $i_L = |i_i|$  with  $i_i$  the input current (the current on the ac side);  $v_i(t) = \text{sign}(i_i)v_S$  is the voltage measured at the diode bridge output;  $P_0$  represents the output power load, it may be a simple constant power source, it may also include the effect of a load resistance or simply a constant current source;  $C$  and  $L$  are the capacitance and inductance of the circuit, respectively;  $u$ , which takes values in the discrete set  $\{0, 1\}$ , denotes the switch position function and acts as the control input. For the controller design purposes we will consider the averaged model, i.e., the signal  $u$ , originally of discrete nature, will be considered as a continuous signal representing the duty ratio of a PWM switching sequence generated at a relatively high frequency.

The *control objective* is twofold. First, in order to guarantee a power factor near unity, the input current  $i_i$  should follow a signal proportional (same shape and phase) to  $v_S$ , i.e.,

$$i_i \rightarrow i_i^* = g v_S \quad (2)$$

where  $g$  is a gain yet to be defined. This gain represents the conductance of the equivalent resistor seen by the voltage source for a given load  $P_0$  under a unitary power factor functioning.

Second, the dc component of output  $v_C$  should be driven to some constant desired value  $V_d > V$ . Here and in what follows we consider the dc component as the average of a signal taken over a period of the fundamental, that is,  $\langle x(t) \rangle_0 \triangleq \frac{1}{T} \int_{(t-T)}^t x(\tau) d\tau$ .

We will assume that the system parameters  $L$ ,  $C$  and the load power  $P_0$  are unknown quantities that may vary slowly or in steps due to changes in the system. Moreover, we will assume that the source voltage can be described with Fourier series

$$v_S = \sum_{k \in \mathcal{H}} \rho_k^\top V_{S,k} \quad (3)$$

where

$$\rho_k = \begin{bmatrix} \cos(k\omega t) \\ \sin(k\omega t) \end{bmatrix}, \quad V_{S,k} = \begin{bmatrix} V_{S,k}^r \\ V_{S,k}^i \end{bmatrix}$$

numbers  $V_{S,k}^r, V_{S,k}^i \in \mathbb{R}$  are the  $k^{\text{th}}$  harmonic coefficients of the Fourier series description of the source voltage. They are also assumed unknown constants (or slowly varying) and  $\mathcal{H} = \{1, 2, 3, \dots\}$  is the set of indices of the harmonic components considered. Superscripts  $(\cdot)^r$  and  $(\cdot)^i$  are used to distinguish the coefficients associated with  $\cos(k\omega t)$  and  $\sin(k\omega t)$ , respectively.

### III. CONTROLLER DESIGN

To design a controller that considers a  $v_S$  with harmonic contents we find it more convenient to rewrite the model above using the following coordinate transformations

$$i_i = \text{sign}(i_i) i_L, \quad v_i = \text{sign}(i_i) v_S$$

$$z_2 = \frac{v_C^2}{2}, \quad e = uv_C$$

Thus, in open sets excluding the zero crossing points<sup>1</sup>, i.e.,  $\forall t$  such that  $i_i(t) \neq 0$ , the model can be rewritten as

$$L \frac{d}{dt} i_i = -\text{sign}(i_i) e + v_S \quad (4)$$

$$C \frac{d}{dt} z = e |i_i| - P_0 \quad (5)$$

where  $e$ , the voltage across the transistor, represents the actual control input. Moreover, to accomplish the control objective,  $z$  should be driven towards  $V_d^2/2$ . We will assume that the dynamics of  $i_i$  is much faster than the dynamics of  $z$ , and we will thus treat both dynamics separately for control design purposes.

#### A. Inner control loop

In this subsection we design a controller which guarantees tracking of  $i_i$  towards its desired reference  $i_i^*$  computed as in (2). It is straightforward to show that the following controller stabilizes subsystem (4), and guarantees that  $i_i$  tracks its desired reference  $i_i^*$

$$e = \text{sign}(i_i) \left( -L \frac{d}{dt} i_i^* + v_S + K_1 \tilde{i}_i \right) \quad (6)$$

where  $\tilde{i}_i = i_i - i_{id}$  and  $K_1 > 0$  is a design parameter.

Notice that, both the time derivative of  $i_i^*$  and the parameter  $L$  are required in order to implement the controller above. In what follows we will show how this term can be estimated by means of adaptation using the description of source voltage  $v_S$  in Fourier series (its harmonic components) to simplify this computation.

Using (2) and (3) we can develop the term containing the time derivative as follows

$$L \frac{d}{dt} i_i^* = L (g \dot{v}_S + \dot{g} v_S) = \sum_{k \in \mathcal{H}} \rho_k^\top L (\dot{g} - k\omega g \mathcal{J}) V_{S,k} \quad (7)$$

where we have used the fact that

$$\dot{v}_S = - \sum_{k \in \mathcal{H}} k\omega \rho_k^\top \mathcal{J} V_{S,k}, \quad \mathcal{J} = -\mathcal{J}^\top = \begin{bmatrix} 0 & -1 \\ 1 & 0 \end{bmatrix}$$

Now, we define the vector

$$\Phi_k = L (\dot{g} - k\omega g \mathcal{J}) V_{S,k}, \quad k \in \mathcal{H} \quad (8)$$

which for each  $k \in \mathcal{H}$  practically converges towards a constant<sup>2</sup>. Eq. (7) can be further reduced to

$$L \frac{d}{dt} i_i^* = \sum_{k \in \mathcal{H}} \rho_k^\top \Phi_k$$

<sup>1</sup>We point out that not much attention is given at the zero crossing points ( $i_i = 0$ ) in the control design since, as will be shown later, the controller has no other option than taking a zero value at all these points due to physical limitations.

<sup>2</sup>Ideally  $g$  and  $\dot{g}$  should vary slowly and take constant values in the steady state.

where vector  $\Phi_k$  is unknown. Thus, we propose to use an estimate  $\hat{\Phi}_k$  in the control expression (6) above, this yields the controller

$$e = \text{sign}(i_i) \left( - \sum_{k \in \mathcal{H}} \rho_k^\top \hat{\Phi}_k + v_S + K_1 \tilde{i}_i \right) \quad (9)$$

Subsystem (4) in closed loop with controller (9) yields the following error dynamics

$$L \frac{d}{dt} \tilde{i}_i = \sum_{k \in \mathcal{H}} \rho_k^\top \tilde{\Phi}_k - K_1 \tilde{i}_i \quad (10)$$

where  $\tilde{\Phi}_k \triangleq \hat{\Phi}_k - \Phi_k$ .

To deal with the terms associated with the error signals  $\tilde{\Phi}_k$  we propose the following energy storage function

$$W = \frac{L}{2} \tilde{i}_i^2 + \sum_{k \in \mathcal{H}} \frac{1}{2\gamma_k} \left[ \left( \tilde{\Phi}_k^r \right)^2 + \left( \tilde{\Phi}_k^i \right)^2 \right]$$

whose time derivative along the trajectories of (10) is given by

$$\dot{W} = -K_1 \tilde{i}_i^2 + \tilde{i}_i \sum_{k \in \mathcal{H}} \rho_k^\top \tilde{\Phi}_k + \sum_{k \in \mathcal{H}} \frac{\dot{\tilde{\Phi}}_k^\top \tilde{\Phi}_k}{\gamma_k}$$

which is forced to be negative semidefinite if the error on the estimates is constructed according to the following adaptive law

$$\begin{aligned} \dot{\hat{\Phi}}_k^r &= -\gamma_k \tilde{i}_i \cos(k\omega t), \quad k \in \mathcal{H} \\ \dot{\hat{\Phi}}_k^i &= -\gamma_k \tilde{i}_i \sin(k\omega t), \quad k \in \mathcal{H} \end{aligned}$$

or in a more compact form

$$\dot{\hat{\Phi}}_k = -\gamma_k \tilde{i}_i \rho_k, \quad k \in \mathcal{H} \quad (11)$$

where  $\gamma_k > 0, k \in \mathcal{H}$  are design parameters.

It is easy to see that  $\tilde{i}_i \rightarrow 0$  as  $t \rightarrow \infty$  as long as  $e$  is well defined for all  $t$ . Moreover,  $\tilde{\Phi} \rightarrow 0$  as  $t \rightarrow \infty$  as long as  $\tilde{i}_L \rightarrow 0$ . Unfortunately, as will become clear later, this can only be guaranteed in open sets of time, since  $e$ , which is restricted to take values only in a positive interval, attempts to take negative values at the beginning of every half cycle. This problem can be alleviated if, for instance,  $L$  is chosen very small.

The controller (9) with adaptive laws (11) can be further simplified using the following transformations

$$\begin{aligned} \Psi_k^r &= -\rho_k^\top \hat{\Phi}_k, \quad k \in \mathcal{H} \\ \Psi_k^i &= -\rho_k^\top \mathcal{J} \hat{\Phi}_k, \quad k \in \mathcal{H} \end{aligned}$$

The controller (9) is reduced to

$$e = \text{sign}(i_i) \left( \sum_{k \in \mathcal{H}} \Psi_k^r + v_S + K_1 \tilde{i}_i \right) \quad (12)$$

and the adaptive laws can be rewritten as

$$\begin{aligned} \dot{\Psi}_k^r &= \gamma_k \tilde{i}_i - k\omega \Psi_k^i, \quad k \in \mathcal{H} \\ \dot{\Psi}_k^i &= k\omega \Psi_k^r, \quad k \in \mathcal{H} \end{aligned}$$

Expressing the dynamic extension (the adaptations) in the form of a transfer function  $\tilde{i}_i \mapsto \Psi_k^r$ , since in the controller above only the terms  $\Psi_k^r$  ( $k \in \mathcal{H}$ ) appear, this yields

$$\Psi_k^r = \frac{\gamma_k s}{s^2 + k^2 \omega^2} \tilde{i}_i, \quad k \in \mathcal{H} \quad (13)$$

## B. Outer control loop

Direct substitution of controller (9) and (11) in the second subsystem (5) yields the following system (in terms of the increments of  $z$ )

$$C \dot{\tilde{z}} = -i_i \sum_{k \in \mathcal{H}} \rho_k^\top \hat{\Phi}_k + |i_i| v_i + i_i K_1 \tilde{i}_i - P_0 \quad (14)$$

where  $\tilde{z} = z - \frac{V_s^2}{2}$ .

As pointed out before, we consider that the dynamics of the subsystem (10) are much faster than the dynamics of subsystem (14), and moreover, that the controller  $e$  is bounded, which is true if all terms  $\hat{\Phi}_k$  ( $\forall k \in \mathcal{H}$ ) are bounded. Thus, in a relatively short time, practically  $\tilde{i}_i = 0$  and  $\hat{\Phi} = \Phi$ , and the model reduces to

$$C \dot{\tilde{z}} = -g v_S \sum_{k \in \mathcal{H}} \rho_k^\top \Phi_k + g v_S^2 - P_0$$

where we have used the fact  $\text{sign}(i_i^*) = \text{sign}(v_S)$ .

Moreover, since we are mainly interested in the behavior of the dynamics of the dc component of  $\tilde{z}$ , we should neglect the higher order harmonics at the right hand side of the equation above, this yields

$$C \dot{\tilde{z}} = -\langle g v_S \sum_{k \in \mathcal{H}} \rho_k^\top \Phi_k \rangle_0 + g \langle v_S^2 \rangle_0 - P_0$$

Notice that  $\langle v_S^2 \rangle_0$  is nothing else than the square of the RMS value of  $v_S$ , i.e.,  $v_{S,RMS}^2 = \langle v_S^2 \rangle_0$ .

The first term on the right hand side (RHS) can be rewritten, using (3) and (8), as

$$\begin{aligned} \langle g v_S \sum_{k \in \mathcal{H}} \rho_k^\top \Phi_k \rangle_0 &= \left\langle \sum_{k \in \mathcal{H}} \rho_k^\top g V_{S,k} \cdot \sum_{k \in \mathcal{H}} \rho_k^\top L \dot{g} V_{S,k} \right\rangle_0 \\ &\quad - \left\langle \sum_{k \in \mathcal{H}} \rho_k^\top g V_{S,k} \cdot \sum_{k \in \mathcal{H}} \rho_k^\top L g k \omega \mathcal{J} V_{S,k} \right\rangle_0 \end{aligned} \quad (15)$$

We observe that the second term at the right hand side of (15) will contain the products of orthogonal rotating vectors at the same angular speed, plus harmonics components of higher order, thus its dc component will be zero. On the other hand, the first term on the RHS contains harmonic components of higher order plus products of colinear rotating vectors which will produce squares of sinusoidal functions (and thus a dc component) plus higher order harmonics. Thus (15) is reduced to

$$\langle g v_S \sum_{k \in \mathcal{H}} \rho_k^\top \Phi_k \rangle_0 = L g \dot{g} \sum_{k \in \mathcal{H}} \langle (\rho_k^\top V_{S,k})^2 \rangle_0$$

but notice that  $\langle (\rho_k^\top V_{S,k})^2 \rangle_0 = \frac{|V_k|^2}{2}$  and thus

$$\sum_{k \in \mathcal{H}} \langle (\rho_k^\top V_{S,k})^2 \rangle_0 = v_{S,RMS}^2$$

It is common practice in applications to obtain  $i_i^*$  as follows

$$i_i^* = \frac{G v_S}{v_{S,RMS}^2} \quad (16)$$

this is equivalent to make the following transformation in our developments

$$G = gv_{S,RMS}^2$$

This simple useful transformation keeps the values of most variables on the same order of magnitude, and thus reduces the error in numerical computations. Notice that the value of  $g$  is usually very small.

Finally, the error model can be written as

$$C\dot{\tilde{z}} = -\frac{LG\dot{G}}{v_{S,RMS}^2} + G - P_0 \quad (17)$$

We propose to compute  $G$  as

$$\dot{G} = -K'_i\tilde{z} - K'_p\zeta \quad (18)$$

$$\zeta = \frac{sa}{s+b}\tilde{z} \quad (19)$$

where  $s$  is the complex variable and  $K'_p$ ,  $K'_i$ ,  $a$  and  $b$  are positive design parameters.

The form of this controller is motivated from the form of a simple PI, where  $\zeta$  represents the signal  $\tilde{z}$  filtered by means of a first order filter which is denoted in control literature as the “dirty derivative”. We observed that direct use of  $\tilde{z}$  in the computation of  $g$  (using a normal PI) causes the introduction of more harmonics which will in principle deform the shape of reference  $i_i^*$  causing the degradation of the power factor. The controller (18)–(19) can be rewritten in a more convenient form as follows

$$\dot{G} = -K_i\tilde{z} + K_p\zeta \quad (20)$$

$$\dot{\zeta} = b(\tilde{z} - \zeta) \quad (21)$$

where  $K_i = K'_i + K'_p a$  and  $K_p = K'_p a$ .

It can also be written in the form of a transfer function having as input  $\tilde{z}$  and output  $G$

$$\frac{G}{\tilde{z}} = -\frac{K_i s + (K_i - K_p)b}{s(s+b)}$$

which turns out to be a simple lead–lag type controller plus an integrator.

Let us study now the local stability of the closed loop system composed by (17), (20) and (21). Linearization of these equations around the equilibrium point  $[\tilde{z}, \overline{G}, \overline{\zeta}]^T = [0, P_0, 0]^T$ , gives

$$\begin{bmatrix} \dot{\tilde{z}} \\ \dot{G} \\ \dot{\zeta} \end{bmatrix} = \begin{bmatrix} \frac{LP_0 K_i}{Cv_{S,RMS}^2} & \frac{1}{C} & -\frac{LP_0 K_p}{Cv_{S,RMS}^2} \\ -K_i & 0 & K_p \\ b & 0 & -b \end{bmatrix} \begin{bmatrix} \tilde{z} \\ G \\ \zeta \end{bmatrix} \quad (22)$$

where  $\tilde{G} \triangleq G - \overline{G}$ .

System (22) is stable provided the following conditions on the design parameters are fulfilled

$$K_i > K_p, \quad K_i < \frac{Cv_{S,RMS}^2}{LP_0} \quad (23)$$

$$\frac{Cv_{S,RMS}^2}{LP_0 b} K_p > K_i(C + K_i) \cong K_i^2$$

where the last condition is a little conservative.

Fig. 2 presents a block diagram of the inner control loop integrated by (12), the bank of second order filters (13) and the outer control loop composed by a lead–lag plus integrator filter.

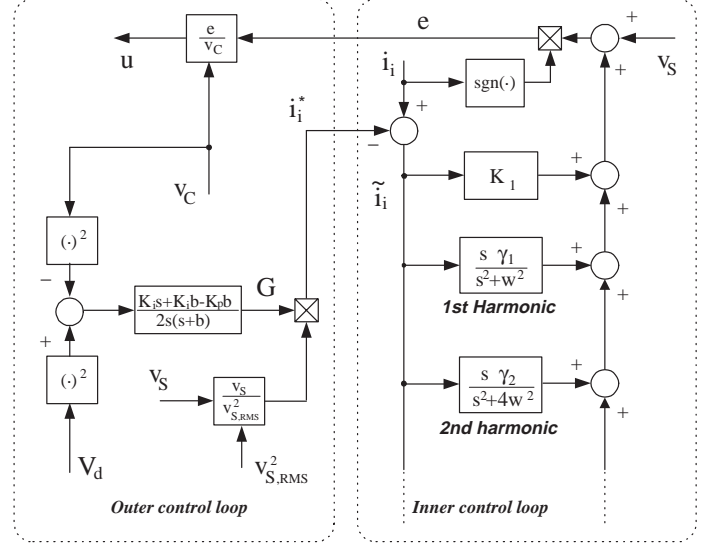


Fig. 2. Block diagram of the proposed controller composed by the inner and outer control loops

#### IV. EFFECTS OF SWITCHING ON THE POWER FACTOR

In this section we study system limitations due to constraints on the control input  $u \in [0, 1]$ . For simplicity we consider a sinusoidal voltage source, i.e.,  $v_S = V \sin(\omega t)$  ( $v_{S,RMS}^2 = V^2/2$ ) and we assume that in the steady state

- $v_C = V_d$ ,
- $i_i = i_i^*$  (at least at the end of every half cycle)
- $g = \frac{2P_0}{V^2}$
- $\hat{\Phi}_1 = [2\omega LP_0/V, 0]^T$

The *equivalent controller*, i.e., the controller that keeps zero tracking error is given by

$$u_{eq} = \frac{V}{V_d} |\sin(\omega t)| - \frac{2\omega LP_0}{V V_d} \text{sign}(\sin(\omega t)) \cos(\omega t) \quad (24)$$

Let us focus only on the first half cycle, i.e.,  $0 \leq \omega t \leq \pi$ . We observe from (24) that  $u_{eq}$  takes negative values at the beginning of each half period. The controller is thus maintained in  $u = 0$  and we can solve for  $i_L$  from (1) considering  $i_L(0) = 0$ , this yields

$$i_L(t) = \frac{V}{\omega L} (1 - \cos(\omega t))$$

The controller is maintained at  $u = 0$  until the trajectory of  $i_L$  reaches the tracking reference signal that occurs at  $\omega t = \beta$

$$\beta = 2 \arctan \left( \frac{2\omega LP_0}{V^2} \right) \quad (25)$$

The trajectory of the inductor current, in steady state, is approximately

$$i_L(t) = \begin{cases} \frac{V}{\omega L} (1 - \cos(\omega t)), & 0 \leq \omega t \leq \beta \\ \frac{2P_0}{V} \sin(\omega t), & \beta < \omega t \leq \pi \end{cases} \quad (26)$$

The *ac-line current*  $i_i(t)$  given by

$$i_i(t) = i_L(t) \text{sign}(\sin(\omega t)) \quad (27)$$

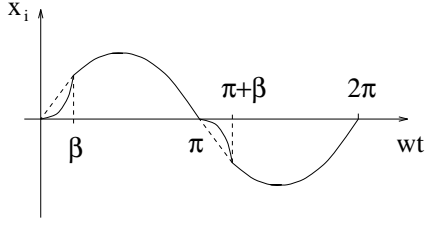


Fig. 3. Input current time response.

has the alternate symmetrical form shown in Fig. 3

Therefore perfect tracking of the current can only be guaranteed in open intervals, remaining thus a pulsating alternate signal on the tracking error  $\hat{i}_i$ .

To avoid possible errors in the estimation of  $\Phi_k$ ,  $k \in \mathcal{H}$  due to the unavoidable pulsating current tracking error, we propose to freeze the adaptation on these intervals, where, as stated before,  $u$  attempts to take negative values. This can be carried out by selecting  $\gamma_k$  as follows

$$\gamma_k = \begin{cases} \gamma_k & , u > 0, k \in \mathcal{H} \\ 0 & , u \leq 0, k \in \mathcal{H} \end{cases} \quad (28)$$

whose effect, according to the actual implementation presented in the point (i) above, consists in disconnecting the second order filters (13) from the controller of Fig. 2.

## V. SIMULATION RESULTS

Computer simulations were performed to evaluate the proposed feedback controller. We used a resistor and a current source as the output load, as shown in Fig. 4 (controller derivation is completely analogous to the case of constant power load). The system parameters were  $L = 1\text{mH}$ ,  $C = 450\mu\text{F}$ . The source voltage is composed of the fundamental, 2<sup>nd</sup> and 3<sup>rd</sup> harmonic

$$v_S(t) = 162.6 \sin(\omega t) - 15 \cos(2\omega t - 0.25) - 10 \cos(3\omega t - 0.2)$$

where  $\omega = 2\pi \times 60 \text{ rad/s}$  and its RMS value is  $v_{S,RMS} = 115.7$ . The desired output voltage is fixed to  $V_d = 400$  Volts with a maximum output power  $P_{0,max} = 250$  W. The design parameters were selected as follows:  $K_1 = 15$ ,  $K'_p = 2.5$  ( $K_p = 3.75$ ),  $K'_i = 0.1$  ( $K_i = 3.85$ ),  $a = 1.5$ ,  $b = 450$ ,  $\gamma_1 = 100$ ,  $\gamma_2 = 200$ ,  $\gamma_3 = 300$ . Notice that these parameters largely fulfill conditions (23).

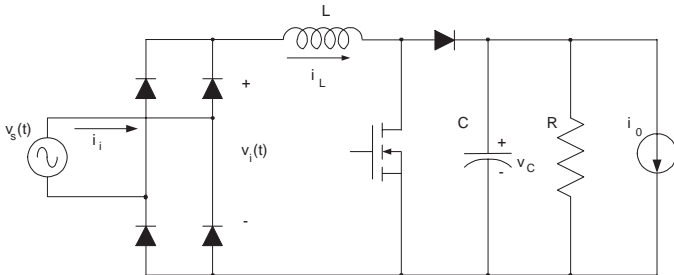


Fig. 4. Simulated circuit.

To test the robustness of the proposed controller against disturbances in the load we have applied a step change in both, the current load and the load resistance. The system starts with  $R = 2000\Omega$  and  $i_0 = 0$  Amp, then at  $t = 1.5$  we change  $R = 2000\Omega$  to  $R = 1000\Omega$  preserving  $i_0 = 0$  Amp, finally at  $t = 3.5\text{sec}$  we introduce  $i_0 = 0.2$  Amp, preserving  $R = 1000\Omega$ .

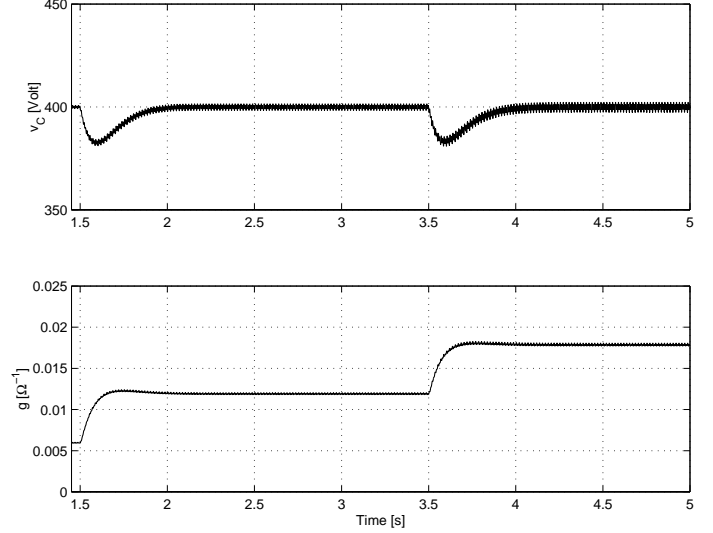


Fig. 5. Time responses for (Top) voltage  $v_C$  and (Bottom)  $g$ , starting with  $R = 2000\Omega$  and  $i_0 = 0$ , then at  $t = 1.5\text{sec}$  we change  $R = 2000\Omega$  to  $R = 1000\Omega$  preserving  $i_0 = 0$  Amp and finally at  $t = 3.5$  we introduce  $i_0 = 0.2$  Amp preserving  $R = 1000\Omega$ .

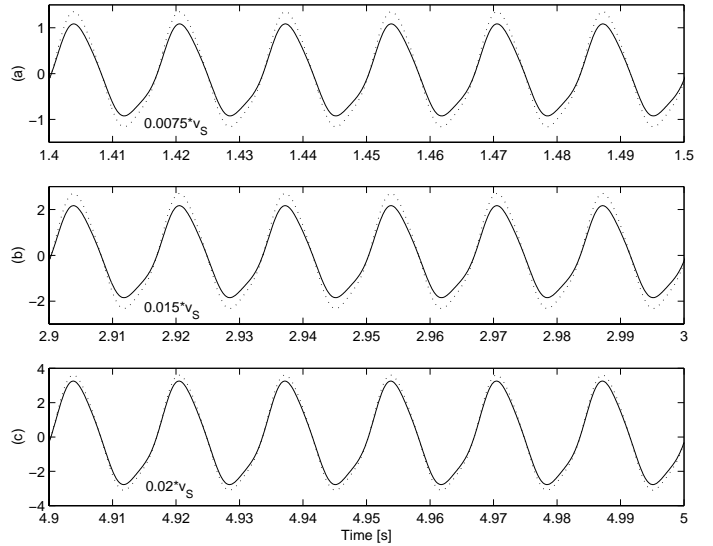


Fig. 6. Current  $i_i(t)$  and scaled  $v_S(t)$  in dotted line, from top to bottom: (a) Starting condition  $R = 2000\Omega$  and  $i_0 = 0$  Amp, (b) Changing load resistance  $R = 1000\Omega$  with  $i_0 = 0$  Amp and (c) Introducing a current  $i_0 = 0.2$  Amp with  $R = 1000\Omega$ .

Fig. 6 shows the time responses of voltage  $v_C$  and the amplitude  $g$  of the reference current under the proposed dissipativity control for the conditions of the test mentioned above. For implementation we have used  $G$  as described before, thus, we have divided  $G$  by  $v_{S,RMS}^2$  to recover  $g$  which appears in Fig. 6. Then

in Fig. 5 we observe the steady state responses of the current  $i_L$  together with the scaled input voltage  $v_S$  for the same three conditions previously mentioned. In Fig. 7 we exhibit the proportional relationship that is established between  $i_i(t)$  and  $v_S(t)$  for the three situations shown in Fig. 5, where the magnitude of the slope coincide with the value of  $g$ , i.e., (a)  $g = 0.006\Omega^{-1}$ , (b)  $g = 0.012\Omega^{-1}$  and (c)  $g = 0.018\Omega^{-1}$ . In Fig. 8 we compare the tracking errors between the proposed controller (top) and a controller where the bank of 2nd order filters are substituted by a conventional PI controller (bottom). We observe that the proposed controller has significantly smaller error; the error observed here is due mainly to the unavoidable distortion at zero crossings. This distortion increases as the load demand increases, as predicted by the analysis.

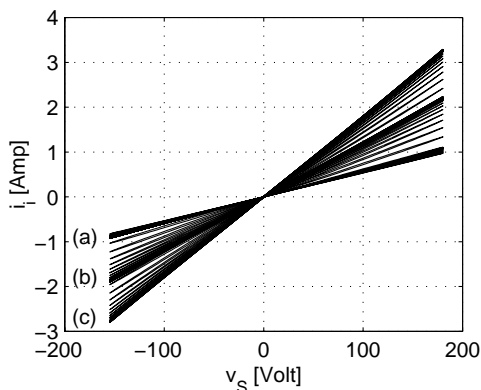


Fig. 7. Current  $i_i(t)$  versus  $v_S(t)$  for the three situations: **(a)** Starting condition  $R = 2000\Omega$  and  $i_0 = 0$  Amp, **(b)** Changing load resistance  $R = 1000\Omega$  with  $i_0 = 0$  Amp and **(c)** Introducing a current  $i_0 = 0.2$  Amp with  $R = 1000\Omega$ .

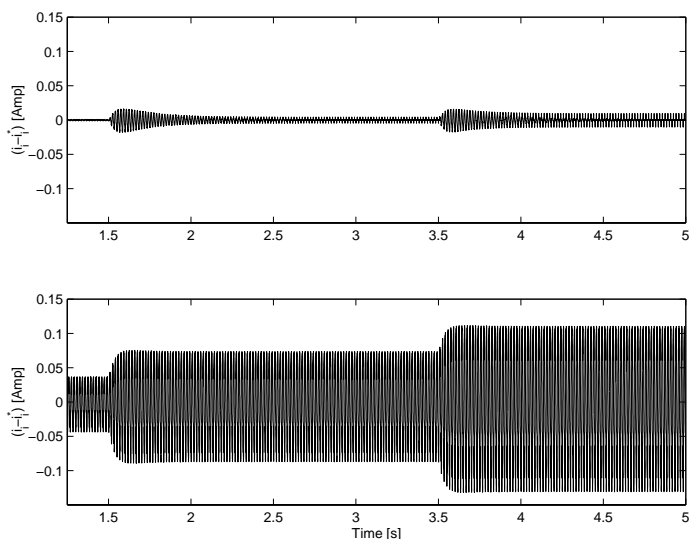


Fig. 8. Current tracking error  $\tilde{i}_i(t)$  for **(Top)** proposed controller and **(Bottom)** replacing the bank of 2nd order filters by a conventional PI.

## VI. CONCLUSIONS

The paper presents an adaptive controller for the power factor precompensator based on boost converter topology. The con-

troller guarantees fast regulation of the output voltage towards a desired constant value with a power factor close to unity. These objectives are fulfilled even in the presence of harmonics on the voltage source and uncertainties on the system parameters and load. The overall controller consists of a cascade interconnection of two compensators, namely the inner and the outer control loop. It is shown that while the latter turns out to be a simple lead-lag plus integration, the former is composed of second order filters tuned at the frequencies of the considered harmonics. Several simulations are provided to assess the performance of the proposed controller.

## REFERENCES

- [1] D. Chevreau and C. Marchand. Pollution harmonique du réseau: comparaison de deux redresseurs monophasés. In *Proc. 9th International Colloquium on CEM*, pages F11–F16, Brest, France, 8–11 June 1998.
- [2] D. Czarkowski and M. K. Kazimierczuk. Energy-conservation approach to modeling PWM DC-to-DC converters. *IEEE Trans. on Aero. and Elect. Syst.*, 29:1059–1063, 1993.
- [3] M. E. Elbuluk, G. C. Verghese, and D. E. Cameron. Nonlinear control of switching power converters. *Control Theory and Advanced Technology*, 5(4):601–617, 1989.
- [4] G. Escobar and H. Sira-Ramirez. A passivity based-sliding mode control approach for the regulation of power factor precompensators. In *Proc. IFAC NOLCOS*, Enschede, The Netherlands, 1998.
- [5] R. Ortega, A. Loria, P. J. Nicklasson, and H. Sira-Ramirez. *Passivity-based control of Euler–Lagrange systems*. Springer-Verlag, 1998.